

1      **Title: Immune correlates of early clearance of *Mycobacterium tuberculosis***  
2      **among tuberculosis household contacts in Indonesia**

4      **Authors:** Todia P. Setiabudiawan<sup>1</sup>, Lika Apriani<sup>2,3</sup>, Ayesha J. Verrall<sup>4</sup>, Fitria Utami<sup>3</sup>, Marion  
5      Schneider<sup>5</sup>, Agnes R. Indrati<sup>3,6</sup>, Pauline P. Halim<sup>7</sup>, Paulina Kaplonek<sup>8</sup>, Hadar Malca<sup>8</sup>, Jessica  
6      Shih-Lu Lee<sup>8</sup>, Simone J.C.F.M. Moorlag<sup>1</sup>, L. Charlotte J. de Bree<sup>1</sup>, Vera P. Mourits<sup>1</sup>, Leo A.B.  
7      Joosten<sup>1,9</sup>, Mihai G. Netea<sup>1,10</sup>, Bachti Alisjahbana<sup>3,11</sup>, Ryan P. McNamara<sup>8</sup>, Galit Alter<sup>8</sup>, Arjan  
8      van Laarhoven<sup>1</sup>, James E. Ussher<sup>5</sup>, Katrina Sharples<sup>12</sup>, Valerie A. C. M. Koeken<sup>1,13</sup>, Philip C.  
9      Hill<sup>14</sup>, Reinout van Crevel<sup>1,15\*</sup>

10     **Affiliations:**

11     <sup>1</sup>Department of Internal Medicine and Radboud Center of Infectious Diseases (RCI), Radboud  
12     University Medical Center; Nijmegen, the Netherlands

13     <sup>2</sup>Department of Public Health, Faculty of Medicine, Universitas Padjadjaran; Bandung,  
14     Indonesia

15     <sup>3</sup>Research Center for Care and Control of Infectious Diseases, Universitas Padjadjaran; Bandung,  
16     Indonesia

17     <sup>4</sup>Department of Pathology and Molecular Medicine, University of Otago; Dunedin, New Zealand

18     <sup>5</sup>Department of Microbiology and Immunology, University of Otago; Dunedin, New Zealand

19     <sup>6</sup>Department of Clinical Pathology, Faculty of Medicine, Universitas Padjadjaran; Bandung,  
20     Indonesia.

21     <sup>7</sup>Faculty of Medicine, Universitas Indonesia; Jakarta, Indonesia

22     <sup>8</sup>Ragon Institute of MGH, MIT and Harvard; Cambridge, Massachusetts, USA

23     <sup>9</sup>Department of Medical Genetics, Iuliu Hatieganu University of Medicine and Pharmacy; Cluj-  
24     Napoca, Romania

25     <sup>10</sup>Department of Immunology and Metabolism, Life and Medical Sciences Institute, University  
26     of Bonn; Bonn, Germany

27     <sup>11</sup>Department of Internal Medicine, Faculty of Medicine, Universitas Padjadjaran; Bandung,  
28     Indonesia

29     <sup>12</sup>Department of Mathematics and Statistics, University of Otago; Dunedin, New Zealand

30     <sup>13</sup>Research Centre Innovations in Care, Rotterdam University of Applied Sciences, the  
31     Netherlands

32     <sup>14</sup>Centre for International Health, University of Otago; Dunedin, New Zealand

33     <sup>15</sup>Centre for Tropical Medicine and Global Health, Nuffield Department of Medicine, University  
34     of Oxford; Oxford, UK

35     \*Corresponding author. Email: Reinout.vanCrevel@radboudumc.nl

36     **One Sentence Summary:** Absence of IGRA conversion among heavily exposed TB contacts is  
37     associated with BCG vaccination and altered innate immune cell phenotype and function.

38 **Abstract:** Some individuals, even when heavily exposed to an infectious tuberculosis patient, do  
39 not develop a specific T-cell response as measured by interferon-gamma release assay (IGRA).  
40 This could be explained by an IFN- $\gamma$ -independent adaptive immune response, or an effective  
41 innate host response clearing *Mycobacterium tuberculosis* (*Mtb*) without adaptive immunity. In  
42 heavily exposed Indonesian tuberculosis household contacts (n=1347), a persistently IGRA  
43 negative status was associated with presence of a BCG scar, and - especially among BCG-  
44 vaccinated individuals - with altered innate immune cells dynamics, higher heterologous  
45 (*Escherichia coli*-induced) proinflammatory cytokine production, and higher inflammatory  
46 proteins in the IGRA mitogen tube. Neither circulating concentrations of *Mtb*-specific antibodies  
47 nor functional antibody activity associated with IGRA status at baseline or follow-up. In a cohort  
48 of adults in a low tuberculosis incidence setting, BCG vaccination induced heterologous innate  
49 cytokine production, but only marginally affected *Mtb*-specific antibody profiles. Our findings  
50 suggest that a more efficient host innate immune response, rather than a humoral response,  
51 mediates early clearance of *Mtb*. The protective effect of BCG vaccination against *Mtb* infection  
52 may be linked to innate immune priming, also termed 'trained immunity'.

53 **Main Text:**

## 54 INTRODUCTION

55 Some people who are heavily exposed to an infectious tuberculosis patient do not  
56 develop evidence of an antigen-specific T-cell response, as measured with an interferon gamma  
57 release assay (IGRA). We have previously found that approximately one quarter of heavily  
58 exposed tuberculosis household contacts in Indonesia do not develop a positive IGRA during  
59 three months follow-up (1). One might argue that these individuals either clear inhaled  
60 *Mycobacterium tuberculosis* (*Mtb*) through a protective innate host response, or that they  
61 develop an IFN- $\gamma$ -independent adaptive immune response.

62 Interestingly, tuberculosis household contacts with a BCG-scar showed a ~50% lower  
63 risk of IGRA conversion compared to unvaccinated individuals (1). BCG protection decreased  
64 with increasing *Mtb* exposure, and correlated with the heterologous innate immune response (2).  
65 These data suggest that BCG-induced innate immune priming (also termed 'trained immunity'),  
66 which has shown to protect against *Mtb* in experimental models (3–5), may clear inhaled *Mtb*  
67 before an adaptive immune response (as measured with an IGRA) can develop.

68 Rather than reflecting protective innate immune clearance, a persistently negative IGRA-  
69 status among heavily exposed household contacts might also be explained by an IFN- $\gamma$ -  
70 independent adaptive immune response. In Uganda, contacts who had tested IGRA- and  
71 tuberculin skin test (TST)-negative over several years (so-called 'resisters'), had detectable IFN-  
72  $\gamma$ -negative T-cell responses to ESAT6/CFP10, the antigens used for IGRA-testing and absent in  
73 BCG (6). They also had similar concentrations of IgG, IgM and IgA antibodies to different *Mtb*  
74 antigens as IGRA-positive contacts (6). Other studies, in humans (7) as well as primates (8),  
75 have also found in anti-*Mtb* antibodies, and suggested that they may protect against *Mtb*  
76 infection as well TB disease (9) in an IFN- $\gamma$ -independent way.

77 To improve our understanding of the correlates of protection against *Mtb* infection, we  
78 examined innate immune cell phenotype and function, and a broad range of anti-*Mtb* specific  
79 antibody features in heavily exposed tuberculosis household contacts in Indonesia, as well as in  
80 BCG-vaccinated adults in a low-TB incidence setting.

81 **RESULTS**

82 **Subhead 1: Characteristics of tuberculosis household contacts in Indonesia**

83 Among 1347 heavily exposed tuberculosis household contacts, after exclusion of  
84 individuals with active TB, 780 (57.9%) had a positive and 433 (32.1%) had a negative IGRA  
85 result at baseline. Baseline IGRA positive individuals had spent more time with the index  
86 patient, and more often slept in the same room as them (**Table 1**). Among household contacts  
87 with a negative IGRA at baseline, 116 (26%) converted to a positive IGRA at 14 weeks. IGRA  
88 conversion was associated with higher exposure, while a persistently IGRA negative status was  
89 associated with the presence of a BCG scar (RR 0.56 [95% CI, 0.40 - 0.77];  $P<0.001$ , **Table S1**).  
90 To strengthen the phenotypes, a strict cut-off value was used for negative IGRA results (<0.15  
91 IU/mL) and conversion to a positive IGRA result at 14 weeks ( $>0.7$  IU/mL). Using these stricter  
92 criteria, we compared 51 participants classified as IGRA converters and 237 as persistently  
93 IGRA-negative individuals (**Fig. S1, Table S1**). Using these IGRA cut-offs, differences between  
94 IGRA converters and persistently IGRA-negative individuals in the level of exposure to the  
95 index patient, and in the proportion of individuals with a BCG scar (RR 0.35 [95%CI, 0.21 -  
96 0.58];  $P<0.001$ , **Table S1**) were more pronounced. Also, IGRA conversion was more among  
97 HHCs of index patients with *Mtb* Beijing genotype strains isolated from sputum compared to  
98 those infected with other genotype strains, and BCG vaccination appeared less protective against  
99 infection by Beijing strains (*10*). Using stricter IGRA criteria, we saw a stronger relative risk  
100 (RR) for infection after exposure to Beijing versus other genotype strains (RR 1.84 [95% CI,  
101 1.11-2.97],  $P=0.015$  with strict criteria vs RR 1.44 [95% CI, 0.98-2.10],  $P<0.001$  with the  
102 manufacturer IGRA criteria, **Table S2A**). Similarly, the genotype-dependent difference in  
103 protection conferred by BCG vaccination was stronger with stricter IGRA cut-offs (**Table S2B**).

104 **Subhead 2: Different dynamics of innate immune cells in IGRA negative contacts**

105 Among a subset of household contacts with a negative IGRA at baseline that had given  
106 informed consent for an additional blood draw at week 2 and week 14 (N=102), 16 different  
107 innate immune cell subsets were measured using flow cytometry. For further analysis we  
108 included participants who had data for both time points, including 22 IGRA converters and 48  
109 persistently IGRA-negative individuals. At week 2, there were no statistically significant  
110 differences in innate immune cell numbers between groups (**Fig. S2**). When results at week 2  
111 and week 14 were compared, innate immune cell numbers showed no statistically significant  
112 change in IGRA converters, while persistently IGRA-negative individuals showed a significant  
113 reduction in the numbers of CD14<sup>hi</sup>CD16<sup>-</sup> classical monocytes, CD14<sup>hi</sup>CD16<sup>+</sup> intermediate  
114 monocytes, CD14<sup>low</sup>CD16<sup>+</sup> non-classical monocytes, CD16<sup>+</sup> mature granulocytes, CD16<sup>dim</sup>  
115 immature granulocytes, and V $\delta$ 2 $^{-}$   $\gamma$  $\delta$  T cells (**Fig. 1B**). When analysis was restricted to  
116 persistently IGRA-negatives contacts, the decrease in numbers of total monocytes, classical  
117 monocytes, intermediate monocytes, non-classical monocytes, mature granulocytes, and V $\delta$ 2 $^{-}$   $\gamma$  $\delta$   
118 T cells was more pronounced among individuals with a BCG scar (N=38) compared to those  
119 without (N=10) (**Fig. 1C**), while this subgroup of persistently IGRA-negative individuals with a  
120 BCG scar also showed a significant reduction in CD56<sup>dim</sup> NK cells (**Fig. S3, Fig. 1C**).

121 **Subhead 3: Association of innate cytokine production with IGRA status**

122 We next examined how innate immune markers correlated with IGRA status (**Fig. 2A**).  
123 First, we compared baseline production of TNF, IL-8, IL-6, IL-1 $\beta$ , IL-1Ra, and IL-10 upon  
124 stimulation with *Mtb*, BCG, and with *E. coli* as a heterologous stimulus. As expected, baseline

125 IGRA-positive individuals (N=145) showed higher cytokine production upon *Mtb* and BCG  
126 stimulation compared to baseline IGRA-negative individuals (N=328) (**Fig. 2B, 2C**). Also,  
127 logistic regression showed a strong association of the innate cytokine production after both *Mtb*  
128 and BCG stimulation with IGRA positivity at baseline. (**Fig. 2D**). Among baseline IGRA-  
129 negative individuals, those who remained IGRA-negative after 14 weeks (N=237) showed higher  
130 innate cytokine production upon *E. coli* stimulation compared to those whose IGRA –converted  
131 to positive (N=91) (**Fig. 2B, 2C, Table S3**), and logistic regression showed IL-6 and IL-8  
132 production upon *E. coli* stimulation to be associated with persistently IGRA-negativity at follow-  
133 up (**Fig. 2E**). Interestingly, the association of *E. coli*-induced production and persistently IGRA-  
134 negativity at follow-up was stronger in contacts with a BCG scar compared to those without for  
135 IL-8, TNF and IL-6 (**Fig. 2F**).

136 **Subhead 4: Associations of baseline IGRA supernatant inflammatory proteins with IGRA**  
137 **status at follow-up**

138 Building on the ex-vivo cytokine production data, we measured inflammatory proteins in  
139 supernatants of baseline IGRA nil and mitogen tubes. Several proinflammatory proteins (ADA,  
140 MCP-3 [CCL7], TWEAK, IL-17C, and IL-18) showed significantly higher concentrations  
141 (logistic regression with adjustment for age, sex, BMI, and exposure risk score) in baseline  
142 IGRA supernatants of contacts whose IGRA remained negative compared to those whose IGRA  
143 converted to positive at 14 weeks (**Fig 3A**). Differentially abundant proteins showed consistent  
144 results in nil and mitogen tubes (**Fig 3B**). Besides the aforementioned proteins, 5 additional  
145 inflammatory proteins in mitogen-stimulated IGRA supernatants (CSF-1, CD244, DNER, CD6,  
146 and VEGFA) correlated with IFN- $\gamma$  (TBAg – Nil) levels at 14 weeks after adjustment for age,  
147 sex, BMI, and exposure risk score (**Fig 3D**).

148 **Subhead 5: Antibodies and antibody function in relation to IGRA status**

149 Antibodies were measured at baseline in randomly selected IGRA-positive (n=100) and  
150 all IGRA-negative contacts (N=433). Similar to the larger cohort, IGRA-positive individuals had  
151 higher exposure to the index case, and (by definition) higher quantitative IGRA results (**Table**  
152 **S2**). After filtering for antibodies with concentrations higher than those measured in PBS, 25 out  
153 of 55 *Mtb*-antigen specific antibody isotypes were selected for analysis (**Fig. S4**). Antibodies  
154 showed a moderate association with age, sex and BMI (**Fig. S5A**). No antibodies measured at  
155 baseline were significantly different between IGRA-positive and IGRA-negative individuals  
156 (**Fig. 4A**). Partial least squares – discriminant analysis (PLS-DA) showed overlapping clusters of  
157 IGRA-positive and IGRA-negative individuals (**Fig. 4B**). Also, no antibody levels were  
158 associated with IGRA status at baseline based on logistic regression analysis adjusting for age,  
159 sex, and BMI, and correction for multiple testing (**Fig. 4C**).

160 We next examined if antibodies against *Mtb* measured at baseline were associated with  
161 risk of IGRA-conversion, using strict IGRA cut-off criteria. No antibodies were significantly  
162 different between persistently IGRA-negative individuals (N=237) and IGRA converters (N=51;  
163 **Fig. 4D**). PLS-DA showed no differences between the groups (**Fig. 4E**). In addition, no  
164 antibodies were associated with the risk of IGRA conversion in logistic regression (**Fig. 4F**).  
165 Moreover, when analysis was limited to household contacts with a BCG-scar, no differences  
166 between groups were found in antibody concentrations (data not shown).

167                   Antibodies can exert their function through lysis of infected cells by complement  
168 activation, or promote cellular or neutrophil phagocytosis, which might add to clearance of *Mtb*  
169 upon exposure. Focusing on LAM-specific antibodies which had the highest variable of  
170 importance projection scores in the PLS-DA (**Fig. S6**), we examined if antibody-dependent  
171 complement deposition (ADCD), antibody-dependent cellular phagocytosis (ADCP), and  
172 antibody-dependent neutrophil phagocytosis (ADNP) were associated with IGRA conversion.  
173 Using our stricter IGRA criteria and a subset of individuals matched for age and sex, IGRA  
174 converters (N=50) had higher MFI for LAM-dependent ADCD than persistently IGRA-negative  
175 individuals (N=50), while ADCP and ADNP showed no difference based on univariate testing  
176 (**Fig. S7A**). However, in logistic regression adjusting for age, sex, and BMI, there was no  
177 association between ADCD, ADCP, or ADNP with IGRA status during follow-up (**Fig. S7B**).

#### 178 **Subhead 6: Effect of BCG vaccination on cytokine production and anti-*Mtb* antibodies**

179                   To further investigate the induction of innate immune responses and antibody production  
180 after mycobacterial stimulation *in vivo*, we next used a cohort of healthy volunteers vaccinated  
181 with BCG in a low-TB incidence setting (11). We purposely selected a low burden setting, to  
182 look at the effect of BCG vaccination – which had shown strong relations with immune markers  
183 in the high burden setting – avoiding confounding by exposure to *M. tuberculosis*.

184                   As expected, BCG vaccination led to an increase in ex vivo *Mtb*-induced IFN- $\gamma$   
185 production, but also to an increase in innate cytokines (**Fig. 5A**). As previously shown, BCG  
186 vaccination also led to increased heterologous cytokine production, although not in all  
187 individuals, as depicted for stimulation with *Staphylococcus aureus* in **Fig. 5B**. To examine a  
188 possible effect of BCG vaccination on anti-*Mtb* antibodies, we measured concentrations of 5  
189 antibody isotypes and binding level of 2 Fc-receptors, to 9 *Mtb* antigens standardized to HA.  
190 After 90 days, when corrected for multiple testing, several *Mtb*-specific IgG3 showed a  
191 statistically significant, albeit minimal increase, while several *Mtb*-specific IgM antibodies  
192 showed a minimal decrease (**Fig. 5C/D, Fig. S8**).

## 193 **DISCUSSION**

194                   In a tuberculosis household study in Indonesia, approximately one fourth of heavily-  
195 exposed contacts still had a negative IGRA three months after tuberculosis diagnosis of the index  
196 case. Examining their innate immune response as a possible mechanism to remain uninfected,  
197 individuals with a persistently negative IGRA showed a stronger reduction of innate immune  
198 cells over time compared to IGRA converters, and higher heterologous production of cytokines  
199 and inflammatory proteins at baseline. No differences were found in baseline concentration or  
200 function of anti-*Mtb* antibodies, as a possible marker of an IFN- $\gamma$  independent adaptive immune  
201 response. Among contacts with a BCG scar, which was associated with a persistently negative  
202 IGRA status, more pronounced differences were seen in innate immune cell numbers and  
203 function between IGRA converters and persistently IGRA-negative individuals. Furthermore, in  
204 a low-incidence setting, adult BCG vaccination induced heterologous cytokine production, but  
205 did not lead to significant changes in anti-*Mtb* antibodies.

206                   A T cell-mediated IFN- $\gamma$  response is important, but not sufficient for protection against  
207 tuberculosis (12). T-cell mediated interferon- $\gamma$  (IFN- $\gamma$ ) responses against *Mycobacterium*  
208 *tuberculosis* (*Mtb*) antigens are used for diagnosis of *Mtb* infection, with IFN- $\gamma$  release assays  
209 (IGRAs) (13). T-cell immunity is crucial for protection against tuberculosis, as shown by the fact

210 that among people with HIV, loss of CD4 T-cells correlates with the risk of tuberculosis (14). In  
211 addition, rare genetic defects have demonstrated the crucial role of IFN- $\gamma$ -signaling in  
212 mycobacterial infections (15). Nevertheless, high IGRA IFN- $\gamma$  production, as a mirror of T cell-  
213 mediated immunoreactivity against *Mtb*, increases rather than reduces an individual's likelihood  
214 of developing TB disease (16). Also, *Mtb* seems to benefit from T cell recognition, as evidenced  
215 by the hyper-conserved T cell epitope sequences in the *Mtb* genome (17). In addition, the  
216 MVA85A vaccine, which induces robust secretion of IFN- $\gamma$  by CD4+ T cells, showed no  
217 protection against TB disease in clinical trials (18, 19). As such, these studies strongly argue that  
218 innate or other CD4/IFN- $\gamma$ -independent mechanisms are also required for protection against  
219 tuberculosis. It should be noted that the correlates of protection against *Mtb* infection and TB  
220 disease are not necessarily the same.

221 Determining why some individuals do not develop a positive T cell dependent TST or  
222 IGRA despite heavy exposure to *Mtb* can help identify novel correlates of protection against *Mtb*  
223 infection. The terms 'early clearance' (20) and 'resisters' have been used to label this clinical  
224 phenotype (21). We studied early clearance in tuberculosis contacts in the context of a well-  
225 defined exposure within a household, with a relative short follow-up, while so-called resisters are  
226 tuberculosis contacts with negative TSTs and IGRAAs despite living in a high-incidence setting  
227 for years. Early clearance can be defined as a relative, or dynamic, measure of protection against  
228 *Mtb* infection (22), as we and others have shown that it is less common with heavier *Mtb*  
229 exposure (1), or exposure to more virulent Beijing genotype strains (10). In contrast, resisters can  
230 be seen as individuals who do not establish *Mtb* infection despite repeated tuberculosis exposure  
231 of varying intensity over a long period of time (21).

232 Our study on early clearance in tuberculosis household contacts in Indonesia points to a  
233 significant role for innate immunity in the early protective response against *Mtb*. This hypothesis  
234 is supported by the elevated heterologous production of proinflammatory cytokines and  
235 inflammatory proteins, both produced mainly by innate immune cells, in persistently IGRA-  
236 negative individuals. In addition, the reduction in innate cell numbers which was found among  
237 contacts with a repeatedly negative IGRA at follow-up likely reflects the resolution of a  
238 protective innate inflammatory resolution after early clearance of *Mtb*, similar to the decreasing  
239 monocyte to lymphocyte ratio which has been reported during treatment of tuberculosis patients  
240 (23) and after TB preventive therapy of *Mtb* infected individuals (24).

241 The different innate immune cell numbers and function in 'early clearers' in our study  
242 likely reflects a trained immunity (22) endotype associated with rapid elimination of the  
243 mycobacteria. This is further supported by the observation that the differences in innate immune  
244 cell phenotype and heterologous cytokine production between IGRA converters and persistently  
245 IGRA-negative individuals were more pronounced when analysis was restricted to BCG-  
246 vaccinated individuals. These findings mimic those of studies focusing on BCG-induced trained  
247 immunity in tuberculosis. In mice, BCG vaccination induces trained immunity in hematopoietic  
248 stem cells, which upon adoptive transfer conferred protection against *Mtb* in non-vaccinated  
249 mice (3). Similarly, in a macaque model with repeated limiting-dose of *Mtb* challenge,  
250 pulmonary mucosal BCG vaccination induced a stronger trained immunity response (4) and  
251 longer delay of IGRA-conversion compared to intradermal BCG (5). In mice, induction of  
252 trained immunity through beta-glucan administration also protected against *Mtb* (25).  
253 Collectively, this suggests that induction of trained immunity may protect tuberculosis contacts  
254 against *Mtb* infection, and might help development of other interventions to prevent tuberculosis.

255 New vaccines preferably should strengthen innate immune protection that can withstand intense  
256 *Mtb* exposure.

257 There is renewed interest in the possible protective role of antibodies against  
258 tuberculosis. In one study, compared to tuberculosis patients, individuals with latent *Mtb*  
259 infection showed a higher abundance, higher Fc receptor binding, and higher antibody-dependent  
260 cellular cytotoxicity for several *Mtb*-specific antibodies (26). In another study, circulating anti-  
261 *Mtb* antibodies that conferred protection against tuberculosis in mice were found in a proportion  
262 of healthcare workers, but not in tuberculosis patients (27). Also, 40 tuberculosis household  
263 contacts in Uganda who had remained TST and IGRA-negative for several years (so-called  
264 'resisters') were found to have detectable levels of *Mtb*-specific antibodies, similar to 39 *Mtb*  
265 IGRA/TST-positive individuals (6). While in a study in South Africa, 30 TST/IGRA-negative  
266 miners showed lower levels of *Mtb*-specific IgG and lower binding of *Mtb*-specific Fc $\gamma$ R2B and  
267 Fc $\gamma$ R3A compared to 37 TST/IGRA positive individuals (7).

268 In our large study in heavily exposed contacts, *Mtb*-specific antibody features (both  
269 abundance and functionality) were not different when we compared 100 IGRA-positive and 433  
270 IGRA-negative household contacts at time of diagnosis of the index patient. Also, no differences  
271 in baseline antibody features were seen between 51 IGRA converters and 237 persistently IGRA-  
272 negative individuals. The difference between our data and previous studies from the literature  
273 investigating the impact of antibodies could be due to several causes. Differences in the  
274 phenotypes of the participants ('early clearance' versus 'resisters'), our use of stricter IGRA-  
275 criteria to avoid possible misclassification, or our adjustment of antibody concentrations to  
276 control measurements, may provide some explanation. Of note, the presence of a BCG-scar was  
277 associated with protection against IGRA-conversion, and BCG vaccination status interacted with  
278 innate immune correlates in household contacts, but no such relation was found between BCG  
279 vaccination and antibody profiles. Finally, intradermal BCG vaccination of adults in a low-  
280 incidence setting, which has been shown to induce trained immunity and associated with an  
281 enhanced capacity to control mycobacterial growth (28, 29), did not significantly alter titers of  
282 *Mtb*-specific antibodies. This is in line with older studies on BCG vaccination from Sweden,  
283 which showed protection against tuberculosis, but no significant increase in *Mtb*-specific  
284 antibodies (30).

285 Our study has several limitations. Our definition of *Mtb* infection was based on IGRA,  
286 which cannot distinguish mere immunoreactivity from actual infection. However, our primary  
287 comparison was between contacts who remain IGRA-negative after 3 months, and those who  
288 convert to a positive IGRA, likely reflecting new *Mtb* infection from their recent exposure.  
289 IGRA measurements, especially with results around the standard cut-off, also show variation  
290 which could lead to misclassification, but this is unlikely with our stricter cut-offs for a negative  
291 and positive IGRA. Finally, future studies could investigate the kinetics of the immune responses  
292 over a longer period of time.

293 Our study also has clear strengths that allow studying correlates of protection against *Mtb*  
294 infection. We used a large cohort specifically recruited to study early clearance with follow-up of  
295 baseline IGRA-negative household contacts, we had precise estimates of *Mtb* exposure that were  
296 strongly associated with IGRA conversion and protection from BCG, and we examined both  
297 innate immune correlates and antibody features. Our findings on associations with BCG were  
298 reproduced in an independent study on BCG vaccination in a low-incidence setting. Other  
299 strengths include our optimization of signal to noise ratio in antibody measurements through

300 proper filtering of antibody measurements and standardization against the positive control  
301 hemagglutinin, and correction for multiple testing in all analyses.

302 In conclusion, our findings suggest that a more efficient host innate immune response,  
303 rather than a humoral response, mediates early clearance of *Mtb*. The protective effect of BCG  
304 vaccination against *Mtb* infection may be linked to induction of a trained immunity phenotype.  
305 Future studies should examine if induction of trained immunity can help prevention of  
306 tuberculosis in highly-exposed individuals, including in the evaluation of new TB vaccines that  
307 may offer improved protection over BCG.

## 308 MATERIALS AND METHODS

### 309 Study design and participants

310 This study was embedded within a large household contact study (INFECT) which was  
311 conducted in Bandung, Indonesia, between 2014 and 2018 (1). In short, household contacts of  
312 sputum smear-positive TB patients (0.5% of whom were HIV-infected) were eligible if they  
313 were older than 5 years and had had no previous TB. They were screened for active TB using a  
314 symptoms screen, chest X-ray and sputum microscopy and culture. Sociodemographic data and  
315 risk factors for *Mtb* infection were collected, including the level of exposure (1), as measured by  
316 sleeping proximity, time spent with the index patient, and presence of cavities, and sputum  
317 mycobacterial load in the index patient. *Mtb* infection status of contacts was assessed by  
318 QuantiFERON-TB Gold In-Tube (QFT-GIT) IGRA, which was repeated at 14 weeks in those  
319 who were initially IGRA-negative. Based on IGRA results, contacts were first classified as  
320 persistently IGRA-negative individuals and IGRA converters using the manufacturer's cut-off  
321 value for the TB antigen (TBAg) tube (0.35 IU/mL). To strengthen the phenotypes, we applied  
322 stricter definitions of low-negative and high-positive IGRA results, only including individuals  
323 whose baseline IFN- $\gamma$  result (TBAg – nil tube) was <0.15 IU/mL, and whose follow-up IGRA  
324 (TBAg – nil) was either <0.15 IU/mL (persistently IGRA-negative individuals) or >0.7 IU/mL  
325 (IGRA converters). The INFECT study was approved by the Health Research Ethics Committee  
326 of Universitas Padjadjaran Indonesia (14/UN6.C2.1.2/KEPK/PN/2014) and the Southern Health  
327 and Disability Ethics Committee New Zealand (13/STH/132).

328 The BCG vaccination cohort (300BCG) recruited volunteers of Western European  
329 ancestry between April 2017 and June 2018 at the Radboud University Medical Center (11).  
330 Following the acquisition of written informed consent, participants underwent blood collection  
331 and then received a standard 0.1 mL dose of BCG (BCG-Bulgaria, InterVax) administered  
332 intradermally in the left upper arm by a medical doctor. The vaccination process for the study  
333 participants was conducted in groups ranging from 6 to 16 individuals each day. Blood samples  
334 were obtained two weeks and three months post-vaccination with BCG. Participants were  
335 excluded if they had been using systemic medications (excluding oral contraceptives or  
336 acetaminophen), antibiotics within three months prior to the study, a previous BCG vaccination,  
337 a history of tuberculosis, any feverish illness in the four weeks preceding the study, any  
338 vaccinations in the three months before the study, or had a medical history indicating  
339 immunodeficiency. The 300BCG (NL58553.091.16) study was approved by the Arnhem-  
340 Nijmegen Medical Ethical Committee.

### 341 Innate immune cell phenotyping and cytokine production

342 Innate immune cell phenotyping with gating strategy and whole blood cytokine assays  
343 from INFECT cohort were performed as previously described (2). In short, we mixed  
344 heparinized blood with 123Count eBeads, followed by staining with one of three antibody panels  
345 designed to identify monocytes (Panel 1), granulocytes (Panel 1), innate  $\alpha\beta$  T-cells (Panel 2),  
346 natural killer (NK) cells (Panel 2), NK T cells (Panel 3), and  $\gamma\delta$  T-cells subsets (Panel 3). Data  
347 were collected using a FACSCalibur flow cytometer and analyzed using FlowJo software. For  
348 whole blood cytokines, samples were incubated with BCG (Danish strain 1331)  $1 \times 10^5$  CFU/mL  
349 (Statens Serum Institut), *Mtb* 5  $\mu\text{g}/\text{mL}$ , *Streptococcus pneumoniae* (ATCC 49619)  $1 \times 10^6$   
350 CFU/mL, *Escherichia coli*  $1 \times 10^6$  CFU/mL, or culture medium for 24 hours at 37°C.  
351 Supernatants were stored at -80°C until batchwise enzyme linked immunosorbent assay (ELISA)  
352 measurement of tumor necrosis factor (TNF), interleukin (IL) 1 $\beta$ , IL-1Ra, and IL-10 (R&D  
353 Systems), IL-6, and IL-8 (Sanquin).

354 In the 300BCG cohort, PBMC ex vivo stimulation assays were performed as previously  
355 described (11). PBMCs were isolated from EDTA whole blood with Ficoll-Paque (GE  
356 Healthcare) density gradient separation. PBMCs ( $5 \times 10^5$ ) were cultured in a final volume of 200  
357  $\mu\text{L}/\text{well}$  in round-bottom 96-well plates (Greiner) and stimulated with RPMI 1640 (medium  
358 control), heat-killed *M. tuberculosis* H37Rv (5  $\mu\text{g}/\text{mL}$ , specific stimulus), or heat-killed *S.*  
359 *aureus* ( $1 \times 10^6$  CFU/mL, nonspecific stimulus). Supernatants were collected after 24 hours and  
360 7 days of incubation at 37°C and stored at -20°C until analysis. Cytokine levels were measured  
361 at 24 hours (IL-1 $\beta$ , IL-6, and TNF) and 7 days (IFN- $\gamma$ ). Supernatant samples from all time points  
362 for a participant were measured on the same plate to ensure that variation between plates would  
363 not affect the calculated fold changes.

### 364 **IGRA supernatant inflammatory marker measurements**

365 Inflammatory proteins from IGRA supernatant nil and mitogen tube (PHA stimulation)  
366 were measured using the commercially available Olink Proteomics AB Inflammation Panel (92  
367 inflammatory proteins) (Uppsala Sweden). In this assay, proteins are recognized by antibody  
368 pairs coupled to cDNA strands which bind in close proximity, followed by extension by a  
369 polymerase reaction. Quality control was performed by Olink Proteomics with 8% samples not  
370 passing the quality control and subsequently excluded from the analysis. We only analyzed  
371 proteins detected in 75% of individuals. Overall, 67 of the 92 (81.5%) proteins were detected in  
372 at least 75% of the plasma samples and included in the analysis.

### 373 **Antibody measurements**

374 For antibody assays, *Mtb* antigens tested were: purified protein derivative (PPD) (Statens  
375 Serum Institute), Ag85A and B in a 1:1 ratio (BEI Resources Cat#NR-49427 and #NR-53526),  
376 recombinant ESAT-6 (BEI Resources Cat#NR-49424) and CFP-10 (BEI Resources Cat#NR-  
377 49425) in a 1:1 ratio, HspX (BEI Resources Cat#NR-49428), and lipoarabinomannan (LAM)  
378 (BEI Resources Cat#NR-14848). An equal mixture of influenza antigens from  
379 HA1(B/Brisbane/60/2008) and HA1 (A/New Caledonia/20/99) (Immune Technology Corp ITIT-  
380 003-001p and IT-003-B3p) was used as a positive assay control.

381 A Luminex assay was used to quantify the relative levels of antigen-specific antibody  
382 isotypes and subclasses and their ability to bind Fc receptors. Luminex Magplex carboxylated  
383 microspheres (Luminex Corporation) were coupled to proteins/antigens via covalent N-  
384 hydroxysuccinimide (NHS)-ester linkages by 1-ethyl-3-(3-dimethylaminopropyl)carbodiimide  
385 hydro-chloride (EDC) and sulfo-NHS per manufacturer recommendations. LAM was modified

386 by 4-(4,6-dimethoxy [1,3,5]triazin-2-yl)-4-methyl-morpholinium (DMTMM) prior to  
387 conjugation. Individual microsphere with unique fluorescence regions allowed for multiplexed  
388 flow cytometry-based quantifications (31).

389 Diluted serum samples were incubated with pooled microspheres for 16 h at room  
390 temperature then washed three times with 0.1% bovine serum albumin (BSA)/0.05% Tween-20  
391 in PBS. Secondary incubations were performed for 2 h at room temperature. Then, samples were  
392 washed three times prior to acquisition. For each assay, median fluorescence intensity (MFI) for  
393 each bead region was measured using an iQue Plus Screener (Intellicyt). For detection of Fc $\gamma$ R-  
394 binding antibodies, diluted serum samples were incubated with the antigen-coated beads as  
395 above. For detection, PE-labeled Streptavidin was coupled to biotinylated, purified Fc $\gamma$ Rs (Duke  
396 Human Vaccine Institute). Excess D-desthiobiotin was used to saturate unbound Strep-PE. The  
397 Strep-Fc $\gamma$ R was then diluted in 0.1 % BSA, 0.05 % Tween-20, and 1X PBS. The blocked  
398 detection reagent was then added as a secondary step similar to above and MFI for each bead  
399 region was quantified using an iQue Plus Screener (Intellicyt)

400 **Data analysis and statistics**

401 All computational analyses were performed in R 4.2.3 with Rstudio integrated  
402 development environment (32, 33). Figures were generated using the R package ‘ggplot2’ or  
403 ‘ggpubr’ unless stated otherwise (34). Tables were made using the R package ‘gtsummary’ (35).

404 To compare cell subpopulations in INFECT cohort across different time periods, the  
405 log<sub>10</sub>-transformed cell counts at 2 weeks and 14 weeks were calculated for each participant.  
406 Unpaired Mann-Whitney U tests were used to compare cell subpopulation between groups at  
407 week 2 (34). Paired Wilcoxon signed rank tests was used for paired significance comparisons of  
408 transformed cell counts in week 2 and week 14(34). Both calculations were adjusted using  
409 Benjamini-Hochberg (false discovery rate). The median fold change and 95% confidence  
410 interval calculated on untransformed cell counts are also presented. The fold change between  
411 IGRA converters and persistently IGRA-negatives was compared using unpaired Mann-Whitney  
412 U test. The same was done to show the median fold change and 95% confidence interval  
413 between persistently IGRA-negative with BCG scar and without BCG scar. A decrease in cell  
414 count is indicated by a fold change of less than 1. The median fold change and confidence  
415 interval were calculated using MedianCI function from ‘DescTools’ R package (36). Paired  
416 Wilcoxon signed rank tests were used and the *P*-value were adjusted for multiple testing using  
417 Benjamini-Hochberg.

418 For cytokine measurements in the INFECT cohort, the level of cytokine that fell below  
419 the detection limit were substituted with the lowest detectable limit for each cytokine (39 pg/mL  
420 for TNF, 19.5 pg/mL for IL-1 $\beta$ , 195 pg/mL for IL-1Ra, 312 pg/mL for both IL-6 and IL-8, and  
421 4.68 pg/mL for IL-10); the highest number for which this was done was for *Mtb* induced TNF  
422 production (3%). Contaminated samples, defined as samples with detectable IL-6 in  
423 unstimulated samples, were removed from the analysis. Cytokine data were log<sub>10</sub> transformed.  
424 Batch effects were removed using the RemoveBatchEffect function from ‘limma’ (37), and  
425 analyses were carried out on the residuals from this model fit. Heatmaps were created using the  
426 ‘ComplexHeatmap’ package (38) visualizing the median Z-score of the batch-adjusted cytokine  
427 variables. Unpaired Mann-Whitney U tests were used to compare adjusted cytokine levels  
428 between groups. Logistic regression was used to estimate the associations between cytokine  
429 production and IGRA status at baseline and follow-up. In the regression model to find the

430 association of cytokine with IGRA status at baseline, we used uncorrected  $\log_{10}$  transformed  
431 cytokine measurements and adjusted for age, sex, BMI, blood monocyte count, blood  
432 lymphocyte count and batch in the formula. While for the association of cytokine with IGRA  
433 status at follow-up, we added exposure risk score as a covariate Odds ratios were calculated from  
434 the beta estimates and adjusted for multiple testing using Benjamini-Hochberg.

435 For inflammatory proteins, only samples and proteins that passed quality control were  
436 used for the analysis. As protein measurements, especially in low concentration, can be affected  
437 by hemolysis, we excluded proteins that might be impacted by hemolysis of less than 3.8g/L  
438 based on the Olink Inflammatory Protein validation data sheet. We also excluded samples that  
439 had hemolysis more than 15g/L (as determined by two researchers blinded to IGRA status  
440 independently visually matching the sample to the hemolysis concentration reference in the  
441 Olink validation data sheet). The inflammatory protein relative levels (NPX) were  $\log_2$   
442 transformed. Logistic regression models were used to estimate the association between NPX  
443 measurement of each inflammatory proteins at baseline and IGRA status at follow-up adjusting  
444 for age, sex, BMI, and exposure score. In addition, linear regression was used to find the  
445 correlation between inflammatory protein level with quantitative IGRA IFN- $\gamma$  (TBAg – Nil)  
446 levels at follow-up.

447 For analysis of antibody profiles, for each individual anti-*Mtb* antibody levels were  
448 divided by the level of hemagglutinin (HA)-specific antibody as a positive control, and the  
449 resulting ratio was  $\log_{10}$  transformed. We established a lower limit of quantification for each  
450 antigen as the mean MFI + 6SD (standard deviation) in the PBS control. For statistical  
451 comparisons of antibody profiles by IGRA status, we used unpaired Mann-Whitney U tests,  
452 corrected for multiple testing by a Benjamini-Hochberg, and showed the fold change in the  
453 heatmap. Supervised clustering using partial least squares discriminant analysis (PLS-DA) using  
454 'mixOmics' package on Z-scored data was used to discriminate the antibody profile explained by  
455 IGRA status, both at baselines and at follow-up (39). Logistic regression models adjusting for  
456 age, sex, and BMI were used to find the associations between baseline antibody levels and IGRA  
457 status at baseline and at follow-up. Functional antibody variables (antibody dependent  
458 complement deposition, antibody-dependent cellular phagocytosis, and antibody-dependent  
459 neutrophil phagocytosis) specific for LAM were compared using the unpaired Mann-Whitney U  
460 tests. In addition, logistic regression adjusting for age, sex, and BMI was used to estimate  
461 associations between antibody functionality and IGRA status at follow-up.

462 In the 300BCG cohort, ex vivo cytokine measurements were  $\log_{10}$  transformed and  
463 corrected for batch effect using linear regression (40). The heatmap of fold change between pre-  
464 vaccination and day 90 post vaccination were shown. Paired Wilcoxon signed rank tests were  
465 used for statistical comparisons of the pre-vaccination and 90-days post vaccination ex vivo  
466 cytokine levels. Antibody MFI were standardized to the MFI of HA-specific antibody as above.  
467 The ratios were then  $\log_{10}$  transformed. The heatmap of fold change of antibody level between  
468 pre-vaccination and 90 days post-vaccination were shown. Paired Wilcoxon signed rank tests  
469 were used for statistical comparisons of the pre-vaccination and 90-days post vaccination.

470

## 471 **List of Supplementary Materials**

472 Fig. S1 to S8

473 Tables S1 to S5

474 Data file S1 (Excel file)

475

## 476 References and Notes

477 1. A. J. Verrall, B. Alisjahbana, L. Apriani, N. Novianty, A. C. Nurani, A. van Laarhoven, J. E.  
478 Ussher, A. Indrati, R. Ruslami, M. G. Netea, K. Sharples, R. van Crevel, P. C. Hill, Early  
479 Clearance of *Mycobacterium tuberculosis*: The INFECT Case Contact Cohort Study in  
480 Indonesia. *The Journal of Infectious Diseases* **221**, 1351–1360 (2020).

481 2. A. J. Verrall, M. Schneider, B. Alisjahbana, L. Apriani, A. van Laarhoven, V. A. C. M.  
482 Koeken, S. van Dorp, E. Diadani, F. Utama, R. F. Hannaway, A. Indrati, M. G. Netea, K.  
483 Sharples, P. C. Hill, J. E. Ussher, R. van Crevel, Early Clearance of *Mycobacterium tuberculosis*  
484 Is Associated With Increased Innate Immune Responses. *J Infect Dis* **221**, 1342–1350 (2020).

485 3. E. Kaufmann, J. Sanz, J. L. Dunn, N. Khan, L. E. Mendonça, A. Pacis, F. Tzelepis, E. Pernet,  
486 A. Dumaine, J.-C. Grenier, F. Mailhot-Léonard, E. Ahmed, J. Belle, R. Besla, B. Mazer, I. L.  
487 King, A. Nijnik, C. S. Robbins, L. B. Barreiro, M. Divangahi, BCG Educates Hematopoietic  
488 Stem Cells to Generate Protective Innate Immunity against Tuberculosis. *Cell* **172**, 176-190.e19  
489 (2018).

490 4. M. P. M. Vierboom, K. Dijkman, C. C. Sombroek, S. O. Hofman, C. Boot, R. A. W.  
491 Vervenne, K. G. Haanstra, M. van der Sande, L. van Emst, J. Domínguez-Andrés, S. J. C. F. M.  
492 Moorlag, C. H. M. Kocken, J. Thole, E. Rodríguez, E. Puentes, J. H. A. Martens, R. van Crevel,  
493 M. G. Netea, N. Aguiló, C. Martin, F. A. W. Verreck, Stronger induction of trained immunity by  
494 mucosal BCG or MTBVAC vaccination compared to standard intradermal vaccination. *CR Med*  
495 **2** (2021), doi:10.1016/j.crm.2020.100185.

496 5. K. Dijkman, C. C. Sombroek, R. A. W. Vervenne, S. O. Hofman, C. Boot, E. J. Remarque, C.  
497 H. M. Kocken, T. H. M. Ottenhoff, I. Kondova, M. A. Khayum, K. G. Haanstra, M. P. M.  
498 Vierboom, F. A. W. Verreck, Prevention of tuberculosis infection and disease by local BCG in  
499 repeatedly exposed rhesus macaques. *Nat Med* **25**, 255–262 (2019).

500 6. L. L. Lu, M. T. Smith, K. K. Q. Yu, C. Luedemann, T. J. Suscovich, P. S. Grace, A. Cain, W.  
501 H. Yu, T. R. McKittrick, D. Lauffenburger, R. D. Cummings, H. Mayanja-Kizza, T. R. Hawn, W.  
502 H. Boom, C. M. Stein, S. M. Fortune, C. Seshadri, G. Alter, IFN- $\gamma$ -independent immune markers  
503 of *Mycobacterium tuberculosis* exposure. *Nature Medicine* **25**, 977–987 (2019).

504 7. L. R. L. Davies, M. T. Smith, D. Cizmeci, S. Fischinger, J. S.-L. Lee, L. L. Lu, E. D. Layton,  
505 A. D. Grant, K. Fielding, C. M. Stein, W. H. Boom, T. R. Hawn, S. M. Fortune, R. S. Wallis, G.  
506 J. Churchyard, G. Alter, C. Seshadri, IFN- $\gamma$  independent markers of *Mycobacterium tuberculosis*  
507 exposure among male South African gold miners. *eBioMedicine* **93** (2023),  
508 doi:10.1016/j.ebiom.2023.104678.

509 8. E. B. Irvine, A. O’Neil, P. A. Darrah, S. Shin, A. Choudhary, W. Li, W. Honnen, S. Mehra, D.  
510 Kaushal, H. P. Gideon, J. L. Flynn, M. Roederer, R. A. Seder, A. Pinter, S. Fortune, G. Alter,  
511 Robust IgM responses following intravenous vaccination with Bacille Calmette–Guérin associate

512 with prevention of *Mycobacterium tuberculosis* infection in macaques. *Nat Immunol* **22**, 1515–  
513 1523 (2021).

514 9. H. A. Fletcher, M. A. Snowden, B. Landry, W. Rida, I. Satti, S. A. Harris, M. Matsumiya, R.  
515 Tanner, M. K. O’Shea, V. Dheenadhayalan, L. Bogardus, L. Stockdale, L. Marsay, A. Chomka,  
516 R. Harrington-Kandt, Z.-R. Manjaly-Thomas, V. Naranbhai, E. Stylianou, F. Darboe, A. Penn-  
517 Nicholson, E. Nemes, M. Hatherill, G. Hussey, H. Mahomed, M. Tameris, J. B. McClain, T. G.  
518 Evans, W. A. Hanekom, T. J. Scriba, H. McShane, T-cell activation is an immune correlate of  
519 risk in BCG vaccinated infants. *Nat Commun* **7**, 11290 (2016).

520 10. A. J. Verrall, L. Chaidir, C. Ruesen, L. Apriani, R. C. Koesoemadinata, J. van Ingen, K.  
521 Sharples, R. van Crevel, B. Alisjahbana, P. C. Hill, INFECT study group, Lower Bacillus  
522 Calmette-Guérin Protection against *Mycobacterium tuberculosis* Infection after Exposure to  
523 Beijing Strains. *Am J Respir Crit Care Med* **201**, 1152–1155 (2020).

524 11. V. A. C. M. Koeken, C. Qi, V. P. Mourits, L. C. J. de Bree, S. J. C. F. M. Moorlag, V.  
525 Sonawane, H. Lemmers, H. Dijkstra, L. A. B. Joosten, A. van Laarhoven, C.-J. Xu, R. van  
526 Crevel, M. G. Netea, Y. Li, Plasma metabolome predicts trained immunity responses after  
527 antituberculosis BCG vaccination. *PLOS Biology* **20**, e3001765 (2022).

528 12. K. Bhatt, S. Verma, J. J. Ellner, P. Salgame, Quest for Correlates of Protection against  
529 Tuberculosis. *Clin Vaccine Immunol* **22**, 258–266 (2015).

530 13. J. Gutierrez, E. E. Kroon, M. Möller, C. M. Stein, Phenotype Definition for “Resisters” to  
531 *Mycobacterium tuberculosis* Infection in the Literature—A Review and Recommendations.  
532 *Frontiers in Immunology* **12** (2021), doi:10.3389/fimmu.2021.619988.

533 14. P. K. Ellis, W. J. Martin, P. J. Dodd, CD4 count and tuberculosis risk in HIV-positive adults  
534 not on ART: a systematic review and meta-analysis. *PeerJ* **5**, e4165 (2017).

535 15. J. Bustamante, S. Boisson-Dupuis, L. Abel, J.-L. Casanova, Mendelian susceptibility to  
536 mycobacterial disease: genetic, immunological, and clinical features of inborn errors of IFN- $\gamma$   
537 immunity. *Semin Immunol* **26**, 454–470 (2014).

538 16. J. R. Ledesma, J. Ma, P. Zheng, J. M. Ross, T. Vos, H. H. Kyu, Interferon-gamma release  
539 assay levels and risk of progression to active tuberculosis: a systematic review and dose-response  
540 meta-regression analysis. *BMC Infect Dis* **21**, 467 (2021).

541 17. I. Comas, J. Chakravarti, P. M. Small, J. Galagan, S. Niemann, K. Kremer, J. D. Ernst, S.  
542 Gagneux, Human T cell epitopes of *Mycobacterium tuberculosis* are evolutionarily  
543 hyperconserved. *Nat Genet* **42**, 498–503 (2010).

544 18. M. D. Tameris, M. Hatherill, B. S. Landry, T. J. Scriba, M. A. Snowden, S. Lockhart, J. E.  
545 Shea, J. B. McClain, G. D. Hussey, W. A. Hanekom, H. Mahomed, H. McShane, MVA85A 020  
546 Trial Study Team, Safety and efficacy of MVA85A, a new tuberculosis vaccine, in infants  
547 previously vaccinated with BCG: a randomised, placebo-controlled phase 2b trial. *Lancet* **381**,  
548 1021–1028 (2013).

549 19. M. Tameris, H. Geldenhuys, A. K. Luabeya, E. Smit, J. E. Hughes, S. Vermaak, W. A.  
550 Hanekom, M. Hatherill, H. Mahomed, H. McShane, T. J. Scriba, The candidate TB vaccine,  
551 MVA85A, induces highly durable Th1 responses. *PLoS One* **9**, e87340 (2014).

552 20. A. J. Verrall, M. G. Netea, B. Alisjahbana, P. C. Hill, R. van Crevel, Early clearance of  
553 Mycobacterium tuberculosis: a new frontier in prevention. *Immunology* **141**, 506–513 (2014).

554 21. J. D. Simmons, C. M. Stein, C. Seshadri, M. Campo, G. Alter, S. Fortune, E. Schurr, R. S.  
555 Wallis, G. Churchyard, H. Mayanja-Kizza, W. H. Boom, T. R. Hawn, Immunological  
556 mechanisms of human resistance to persistent Mycobacterium tuberculosis infection. *Nature  
557 Reviews. Immunology* **18**, 575–589 (2018).

558 22. M. Foster, P. C. Hill, T. P. Setiabudiawan, V. A. C. M. Koeken, B. Alisjahbana, R. van  
559 Crevel, BCG-induced protection against Mycobacterium tuberculosis infection: Evidence,  
560 mechanisms, and implications for next-generation vaccines. *Immunol Rev* **301**, 122–144 (2021).

561 23. T. Adane, M. Melku, G. Ayalew, G. Bewket, M. Aynalem, S. Getawa, Accuracy of  
562 monocyte to lymphocyte ratio for tuberculosis diagnosis and its role in monitoring anti-  
563 tuberculosis treatment: Systematic review and meta-analysis. *Medicine (Baltimore)* **101**, e31539  
564 (2022).

565 24. J. Mayito, D. B. Meya, A. Miriam, F. Dhikusooka, J. Rhein, C. Sekaggya-Wiltshire,  
566 Monocyte to Lymphocyte ratio is highly specific in diagnosing latent tuberculosis and declines  
567 significantly following tuberculosis preventive therapy: A cross-sectional and nested prospective  
568 observational study. *PLOS ONE* **18**, e0291834 (2023).

569 25. S. J. C. F. M. Moorlag, N. Khan, B. Novakovic, E. Kaufmann, T. Jansen, R. van Crevel, M.  
570 Divangahi, M. G. Netea,  $\beta$ -Glucan Induces Protective Trained Immunity against Mycobacterium  
571 tuberculosis Infection: A Key Role for IL-1. *Cell Rep* **31** (2020),  
572 doi:10.1016/j.celrep.2020.107634.

573 26. L. L. Lu, A. W. Chung, T. Rosebrock, M. Ghebremichael, W. H. Yu, P. S. Grace, M. K.  
574 Schoen, F. Tafesse, C. Martin, V. Leung, A. E. Mahan, M. Sips, M. Kumar, J. Tedesco, H.  
575 Robinson, E. Tkachenko, M. Draghi, K. J. Freedberg, H. Streeck, T. J. Suscovich, D.  
576 Lauffenburger, B. I. Restrepo, C. Day, S. M. Fortune, G. Alter, A functional role for antibodies  
577 in tuberculosis. *Cell* **167**, 433-443.e14 (2016).

578 27. H. Li, X. Wang, B. Wang, L. Fu, G. Liu, Y. Lu, M. Cao, H. Huang, B. Javid, Latently and  
579 uninfected healthcare workers exposed to TB make protective antibodies against Mycobacterium  
580 tuberculosis. *Proc Natl Acad Sci U S A* **114**, 5023–5028 (2017).

581 28. S. A. Joosten, K. E. van Meijgaarden, S. M. Arend, C. Prins, F. Oftung, G. E. Korsvold, S. V.  
582 Kik, R. J. W. Arts, R. van Crevel, M. G. Netea, T. H. M. Ottenhoff, Mycobacterial growth  
583 inhibition is associated with trained innate immunity. *J Clin Invest* **128**, 1837–1851 (2018).

584 29. K. E. van Meijgaarden, W. Li, S. J. C. F. M. Moorlag, V. A. C. M. Koeken, H. J. P. M.  
585 Koenen, L. A. B. Joosten, A. Vyakarnam, A. Ahmed, S. Rakshit, V. Adiga, T. H. M. Ottenhoff,  
586 Y. Li, M. G. Netea, S. A. Joosten, BCG vaccination-induced acquired control of mycobacterial

587 growth differs from growth control preexisting to BCG vaccination. *Nat Commun* **15**, 114  
588 (2024).

589 30. M. H. Fusillo, D. L. Weiss, Lack of Circulating Antibodies After BCG Immunization as  
590 Assayed by the Globulin Titration Technique. *Am Rev Tuberc Pulm Dis* **78**, 793–793 (1958).

591 31. X. Tong, R. P. McNamara, M. J. Avendaño, E. F. Serrano, T. García-Salum, C. Pardo-Roa,  
592 H. L. Bertera, T. M. Chicz, J. Levican, E. Poblete, E. Salinas, A. Muñoz, A. Riquelme, G. Alter,  
593 R. A. Medina, Waning and boosting of antibody Fc-effector functions upon SARS-CoV-2  
594 vaccination. *Nat Commun* **14**, 4174 (2023).

595 32. R Core Team, R: A Language and Environment for Statistical Computing (2021) (available  
596 at <https://www.R-project.org/>).

597 33. RStudio Team, RStudio: Integrated Development Environment for R (2020) (available at  
598 <http://www.rstudio.com/>).

599 34. A. Kassambara, *ggpubr: “ggplot2” Based Publication Ready Plots* (2023;  
600 <https://rpkgs.datanovia.com/ggpubr/>).

601 35. D. D. Sjoberg, K. Whiting, M. Curry, J. A. Lavery, J. Larmarange, Reproducible Summary  
602 Tables with the gtsummary Package. *The R Journal* **13**, 570–580 (2021).

603 36. A. Signorell, *DescTools: Tools for Descriptive Statistics* (2024; <https://CRAN.R-project.org/package=DescTools>).

604 37. M. E. Ritchie, B. Phipson, D. Wu, Y. Hu, C. W. Law, W. Shi, G. K. Smyth, limma powers  
605 differential expression analyses for RNA-sequencing and microarray studies. *Nucleic Acids  
606 Research* **43**, e47 (2015).

607 38. Z. Gu, Complex heatmap visualization. *iMeta* **1**, e43 (2022).

608 39. R. F, G. B, S. A, L. C. K-A, mixOmics: An R package for ’omics feature selection and  
609 multiple data integration. *PLoS computational biology* **13**, e1005752 (2017).

610 40. V. A. C. M. Koeken, L. C. J. de Bree, V. P. Mourits, S. J. C. F. M. Moorlag, J. Walk, B.  
611 Cirovic, R. J. W. Arts, M. Jaeger, H. Dijkstra, H. Lemmers, L. A. B. Joosten, C. S. Benn, R. van  
612 Crevel, M. G. Netea, BCG vaccination in humans inhibits systemic inflammation in a sex-  
613 dependent manner. *Journal of Clinical Investigation* **130**, 5591–5602 (2020).

614

615

616 **Acknowledgments:** The authors extend their appreciation to the dedicated teams involved in  
617 fieldwork, laboratory activities, and data management, including the recruitment of the  
618 INFECT cohort. This team comprised Andini Cahya Nurani, Novianti, Deni, Wiwik  
619 Pratiwi Dody Taufik Akbar, Emira Diandini, Dwi Febni Ratnaningsih, Inas Kathina,  
620 Yusak Sastra Atmaja, Nuni Haeruni, Anbarunik Puteri Danthin, Harold Eka Atmaja, Alif  
621 Al Birru, Nopi Susilawati, and Runi Rahmawati. Also, Rachel F. Hannaway who work on  
622 INFECT from Otago University. Special thanks are also due to the TANDEM study

team, especially coordinator Raspati C. Koesoemadinata, Lidya Chadir, Jessi Anisa, and Ria Windyani for their cooperation. Additionally, the authors acknowledge Corina van den Heuvel, Heidi Lemmers, and Helga Dijkstra for their assistance with the ELISA procedures. Also, we would like to extend our thanks to Liesbeth van Emst for her help in Olink measurements. We would also like to thank all volunteers from the 300BCG cohort for participation in the study. AVJ was supported by a New Zealand Health Research Council Clinical Training Research Fellowship. Cohort recruitment was funded by the University of Otago and Mercy Hospital (through an endowment fund and directly), Dunedin, New Zealand. Index case recruitment and investigation was part of the TANDEM project ([www.tandem-fp7.eu](http://www.tandem-fp7.eu)), which is supported by the European Union's Seventh Framework Programme (FP7/2007–2013) under grant agreement number 305279. The IGRA (QuantiFERON) was donated by Qiagen. Flow cytometry analysis was supported by a grant from the Dean's Bequest Fund, University of Otago. RPM and the Systems Serology Laboratory are supported by the generous gifts of Terry and Susan Ragon, and Mark and Lisa Schwartz. RPM receives funding from the global health vaccine accelerator program (GH-VAP) through the Bill and Melinda Gates foundation (INV-001650). RvC was supported by the Royal Netherlands Academy of Arts and Sciences (09-PD-14) and the VIDI grant 017.106.310 of The Netherlands Organization for Scientific Research. MGN was supported by an ERC advanced grant (833247) and a Spinoza grant of The Netherlands Organization for Scientific Research. The figures were created with BioRender. LCJDB was partly funded by a grant to the Research Center for Vitamins and Vaccines (CVIVA) from the Danish National Research Foundation (DNRF108).

#### 646 **Funding:**

647 New Zealand Health Research Council Clinical Training Research Fellowship (AVJ)  
648 University of Otago and Mercy Hospital (through an endowment fund and directly),  
649 Dunedin, New Zealand (AVJ, PCH)  
650 European Union's Seventh Framework Programme (FP7/2007–2013) grant agreement  
651 305279 (AVJ, PCH)  
652 Dean's Bequest Fund, University of Otago (AVJ)  
653 Global health vaccine accelerator program (GH-VAP) through the Bill and Melinda  
654 Gates foundation INV-001650 (RPM)  
655 The Royal Netherlands Academy of Arts and Sciences 09-PD-14 (RvC)  
656 VIDI grant 017.106.310 of The Netherlands Organization for Scientific Research (RvC)  
657 European Research Council (ERC) advanced grant 833247 (MGN)  
658 Spinoza grant of The Netherlands Organization for Scientific Research (MGN)  
659 the Research Center for Vitamins and Vaccines (CVIVA) from the Danish National  
660 Research Foundation DNRF108 (LCJDB)

#### 662 **Author contributions:**

663 Conceptualization: TPS, GA, VACMK, RvC  
664 Methodology: TPS, VACMK, RvC  
665 Data curation: TPS  
666 Formal analysis: TPS, PPH

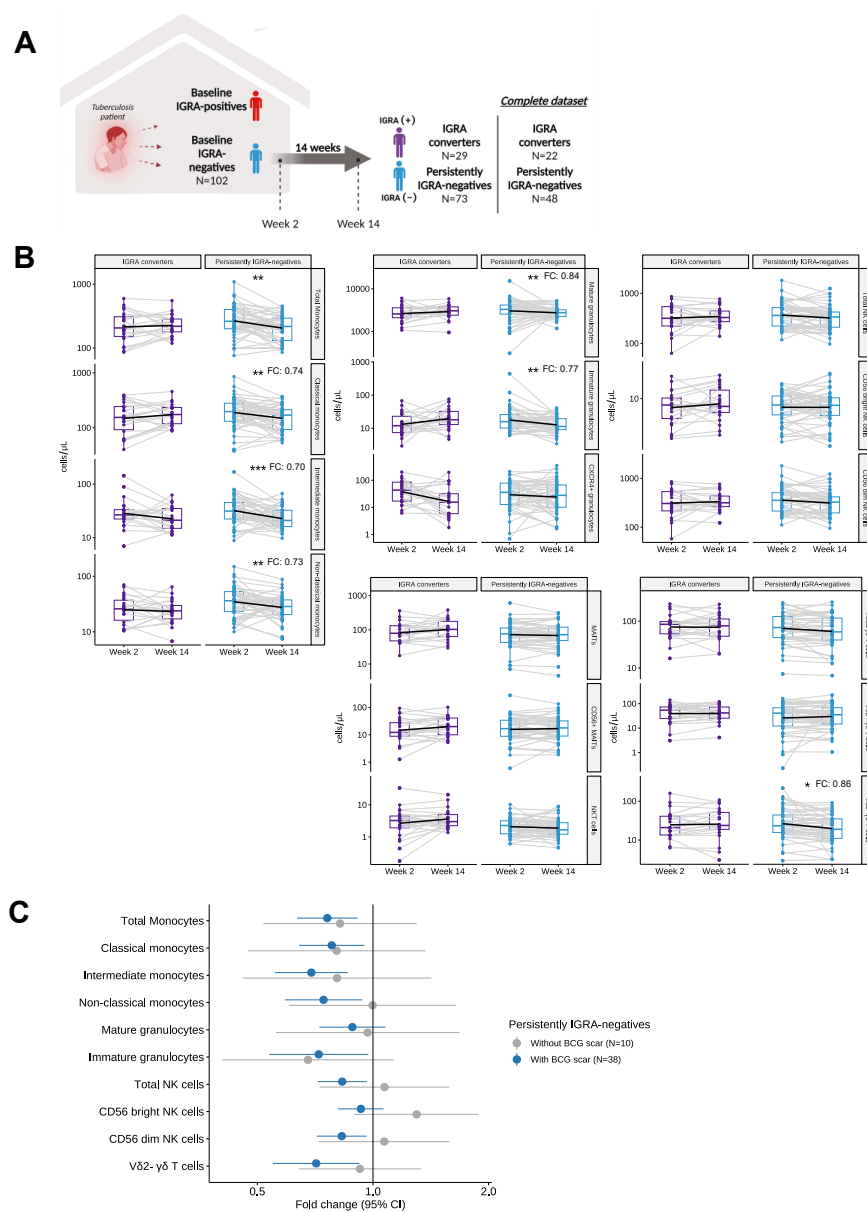
Investigation: TPS, LA, AJV, NN, ACN, ED, FU, RFH, JEU, KS, PK, HM, JSL, VACMK, SJCFMM, LCJDB, VPM, LABJ  
Resources: PCH, BA, RvC  
Writing – original draft: TPS, RvC  
Writing – review & editing: KS, JU, RPM, AvL, LABJ, PCH, MGN, VACMK, RvC  
Visualization: TPS, PPH  
Supervision: MGN, VACMK, RvC

**Competing interests:** Authors declare that they have no competing interests.

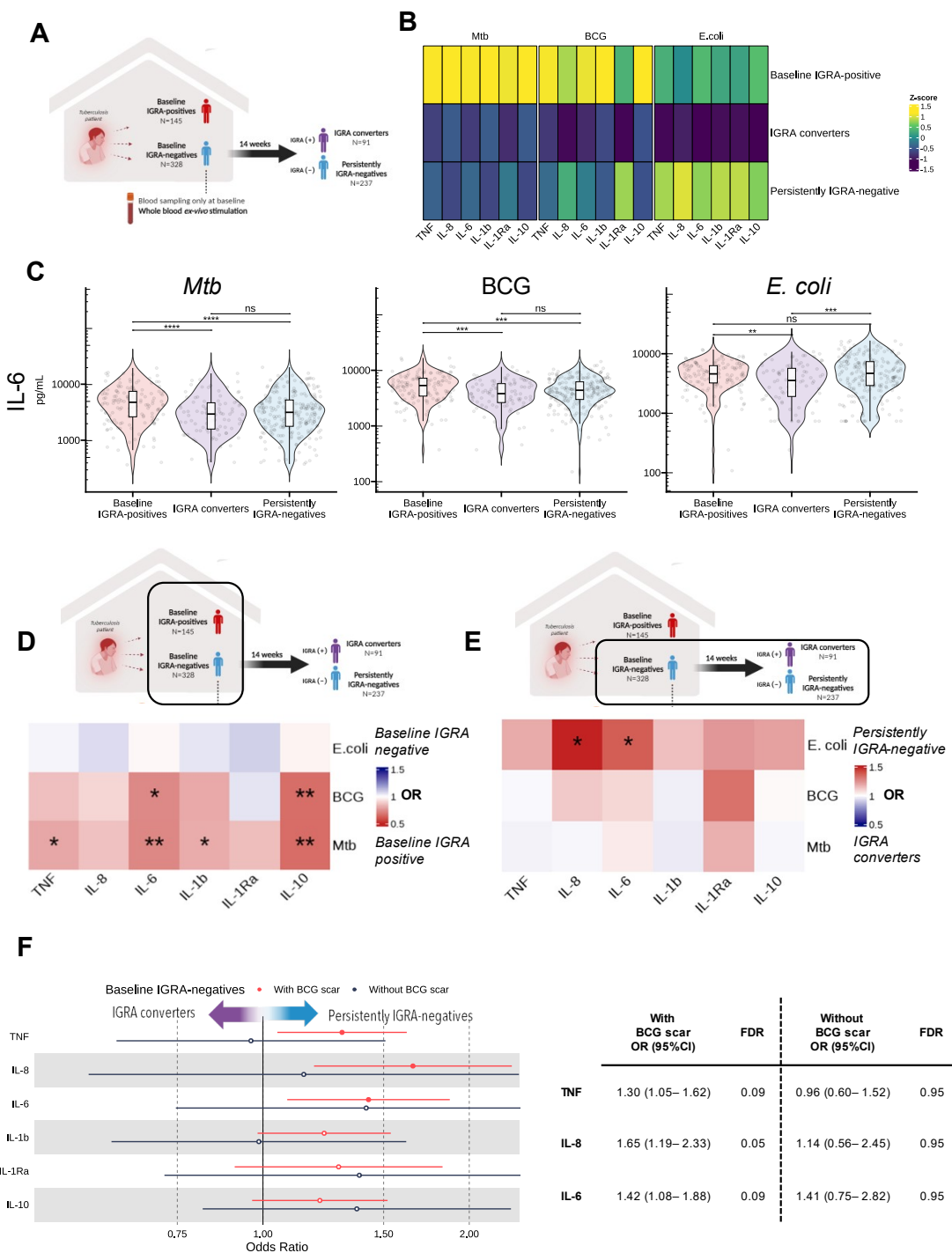
**Data and materials availability:** All data are available in the main text or the supplementary materials.

678

679 **Figures**

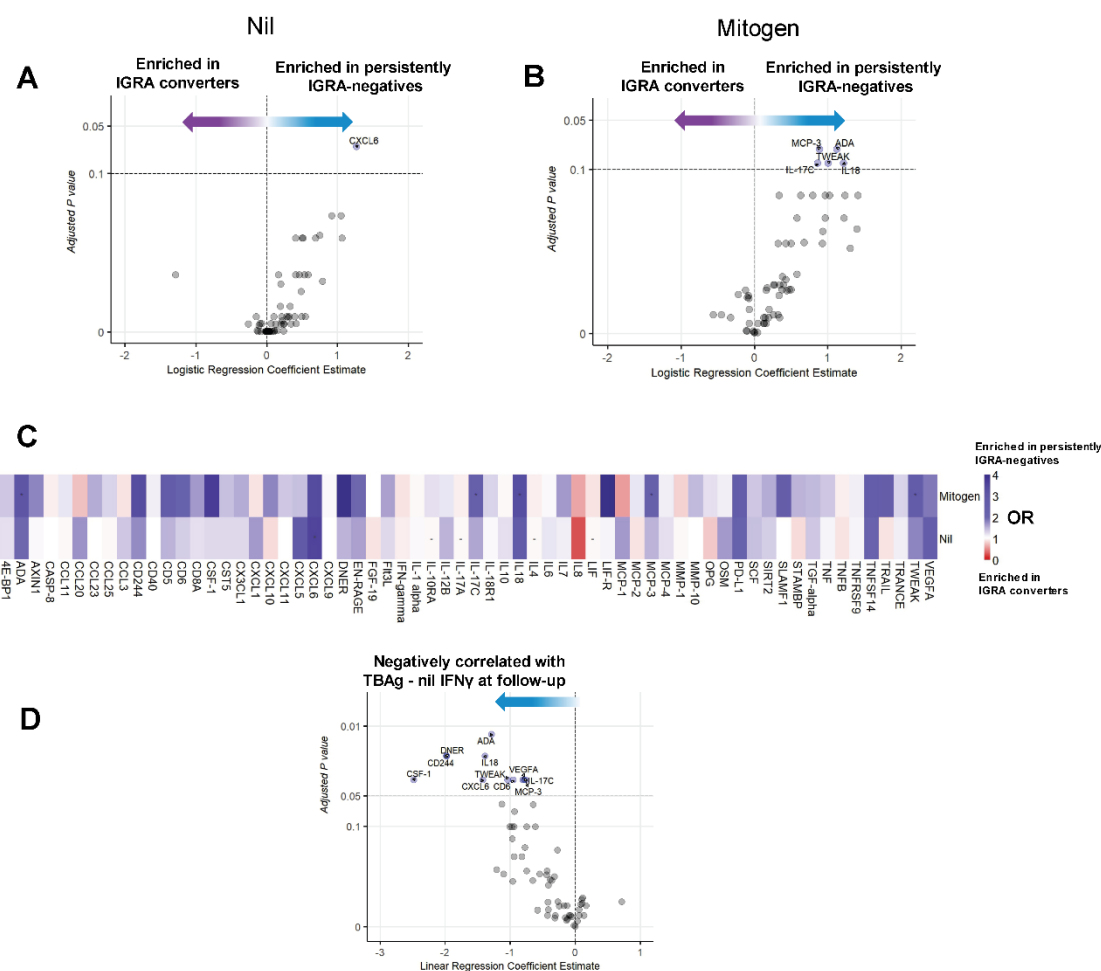


680 **Fig. 1. The dynamics of innate immune cells in IGRA-converters and persistently IGRA-  
681 negative individuals.** (A) Overview of the flow cytometry dataset. (B) Frequencies of  
682 circulating innate immune cells (numbers /  $\mu$ L blood) were compared between week 2  
683 and week 14 in IGRA converters (N=22), and persistently IGRA-negative individuals  
684 (N=48, [FDR<0.1, <0.05, <0.01; \*, \*\*, \*\*\*; FC = median fold change]). (C) Persistently  
685 IGRA-negatives with BCG scar (N=38) showed a larger decrease in cell numbers than  
686 participants without BCG scar (N=10) in the innate circulating immune cells from week 2  
687 to week 14.



689 **Fig. 2. Study outline and ex vivo cytokine production.** (A) Baseline whole blood ex vivo  
690 cytokine production, compared between baseline IGRA-negative (N=328) and IGRA-  
691 positive individuals (N=145), and between IGRA converters (N=91) and persistently  
692 IGRA-negative individuals (N=237). (B) Cytokine production following stimulation with  
693 *Mtb*, BCG, and *E. coli*, with higher *Mtb*-induced cytokine production in baseline IGRA-  
694 positive individuals, and higher *E. coli*-induced production in persistently IGRA-negative  
695 individuals. (C) *Mtb*, BCG, and *E. coli*-induced IL-6 production (as a representative),  
696 stratified for IGRA-status (Mann-Whitney U test after correction for multiple testing).  
697 Association between cytokine production and IGRA status at baseline (D) and 14 weeks  
698 (E), expressed as odds ratio (using logistic regression adjusting for age, sex, BMI,  
699 exposure score, blood monocyte count, blood lymphocyte count, and batch). (F) Relation  
700 between baseline ex-vivo cytokine production (in IGRA-negative individuals) and IGRA  
701 status at 14 weeks, shown as odds ratios, stratified for BCG vaccination status. All  
702 models corrected for multiple testing (Benjamini-Hochberg). (FDR<0.1, <0.05, <0.01,  
703 <0.001; closed circle & \*, \*\*, \*\*\*, \*\*\*\*)

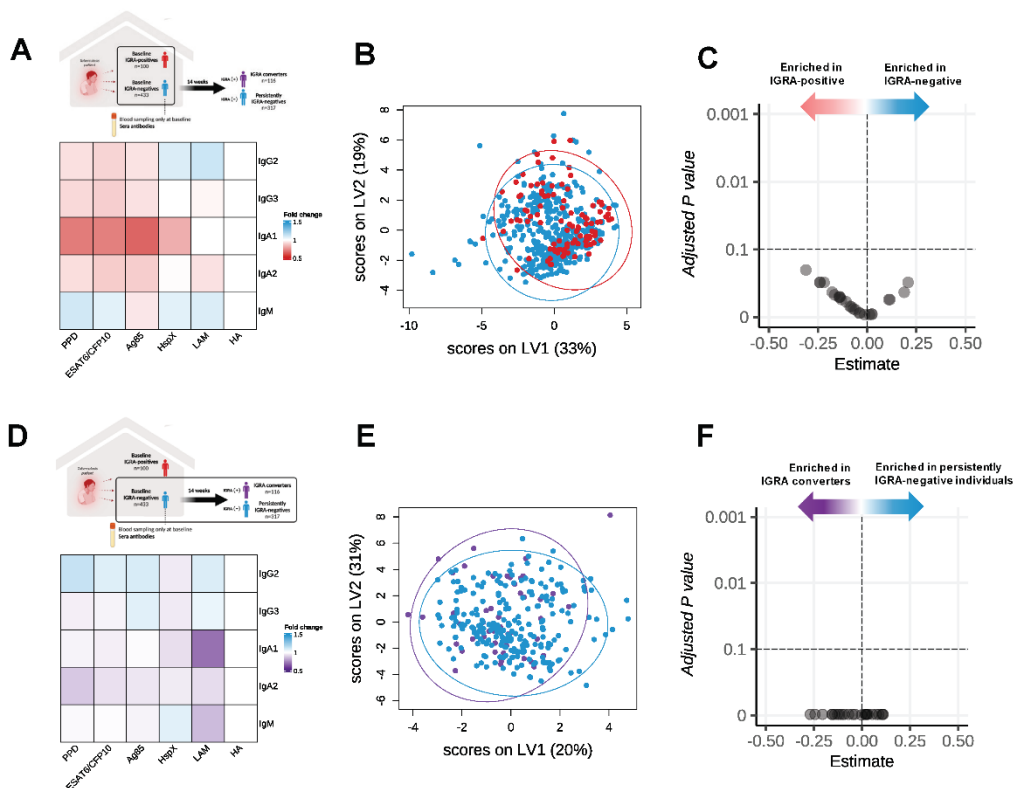
704



705

**Fig. 3. Inflammatory proteins in IGRA supernatants.** Inflammatory proteins relative concentrations (NPX unit, log<sub>2</sub> transformed) in IGRA supernatants (nil and mitogen) at baseline were compared between IGRA converters (N=48) and persistently IGRA-negative individuals (N=128). **(A)** A persistently IGRA-negative status was associated with higher CXCL6 in the baseline IGRA nil tube, and **(B)** with ADA, MCP-3 (CCL7), TWEAK, IL-17C, and IL-18 in the baseline mitogen tube (logistic regression adjusted for age, sex, BMI, and exposure score; FDR<0.1). **(C)** Associations between persistently IGRA-negative status and concentrations of all proteins measured in IGRA nil and mitogen tube (Odds ratios, adjusted for age, sex, BMI, and exposure score). **(D)** In the mitogen tubes, the same proteins, as well as CSF-1, DNER, CD244, and VEGFA, showed a correlation with quantitative TBAg - nil IFN $\gamma$  IGRA results after correction for multiple testing with lower FDR cutoff of 0.05.

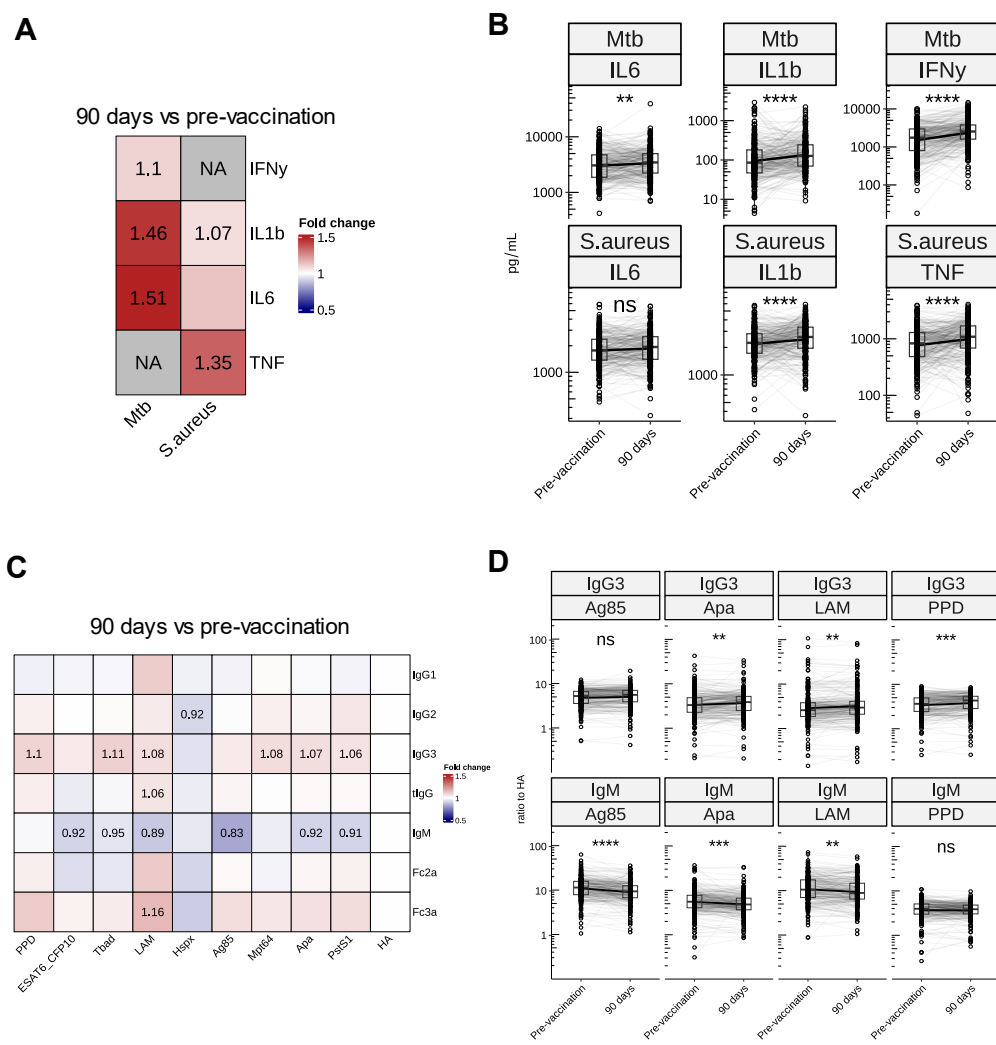
718



719  
720

721 **Fig. 4. Antibody profiles according to IGRA-status at baseline and follow-up.** Antibody  
722 profiles were compared between IGRA-positive (N=100) and IGRA-negative (N=433)  
723 tuberculosis household contacts; and between IGRA converters (N=51) and persistently  
724 IGRA-negative individuals (N=237), based on strict IGRA criteria (<0.15 IU/mL for  
725 negative and >0.70 IU/mL for positive). Fold differences in antibody levels (shown as  
726 ratio of antibodies corrected for the positive control hemagglutinin [HA]), are shown  
727 according to IGRA status at baseline (A; red: higher antibody levels in IGRA-positive  
728 individuals) and follow-up (D; purple: higher antibody levels in IGRA converters). No  
729 difference reached statistical significance, thus, numbers not shown in the heatmap  
730 (Mann-Whitney U test; FDR <0.1). (B) Partial least squares discriminant analysis (PLS-  
731 DA) using the selected 25 antibodies was used to visualize differences in antibody levels  
732 between baseline IGRA-positive (red) and -negative (blue) individuals, and (E) between  
733 IGRA converters (purple) and persistently IGRA-negative individuals (blue). (C) In  
734 logistic regression, no antibody was associated with IGRA status at baseline or follow-up  
735 (F), after adjustment for age, BMI and exposure.

736  
737



738

739 **Fig. 5. Effect of BCG vaccination on cytokine production and Mtb-specific antibodies.**

740 Heatmap showing fold change (A) and the paired boxplot (B) of ex vivo cytokine  
 741 production in Dutch healthy adults (N=298) before and 90 days after BCG vaccination.  
 742 Shown are 24-hour stimulation of PBMCs with *Mtb* and *S. aureus*, and 7-day stimulation  
 743 of *Mtb* for IFN- $\gamma$ . Heatmap showing fold change of hemagglutinin-standardized anti-  
 744 *Mtb* antibody levels at day 90 compared to the pre-vaccination, with statistically  
 745 significant fold changes shown in numbers (C). Changes in IgM and IgG3 antibody  
 746 against different *Mtb* antigens (D). FDR<0.1, <0.05, <0.01, <0.001; \*, \*\*, \*\*\*, \*\*\*\*.

747  
 748

749 **Table 1. Characteristics of tuberculosis household contacts according to baseline IGRA-  
750 status**

751  
752

	Baseline IGRA-positive <sup>a</sup> N = 780	Baseline IGRA-negative <sup>a</sup> N = 433	P value <sup>b</sup>
<b>Case contact characteristics</b>			
Age	31 (17 – 47)	22 (12 – 39)	<0.001
Female sex	58%	53%	0.089
Presence of BCG scar	78%	84%	0.013
Current and previous smoking	35%	31%	0.27
BMI, kg/m <sup>2</sup>	21.6 (18.0 – 25.4)	20.2 (16.8 – 24.4)	0.001
Diabetes <sup>c</sup>	3.2%	3.9%	0.41
<b>Exposure to the index case</b>			
Sleeping in the same room as the index case	30%	20%	<0.001
Waking hours spent with the index case a day before enrollment	5 (2 – 10)	4 (1 – 8)	0.001
Index case highest smear grade			<0.001
Scanty	5.4%	8.3%	
1+	18%	28%	
2+	26%	25%	
3+	50%	38%	
Presence of cavities on chest x-ray of index	56%	44%	<0.001
Extent of x-ray abnormalities	50 (25 – 71)	40 (25 – 59)	<0.001
<i>M. tuberculosis</i> Beijing genotype in the index case	35%	28%	0.022
<b>Blood count parameters at baseline</b>			
Hemoglobin g/dL	13.70 (12.80 – 14.90)	13.70 (12.80 – 15.00)	0.56
Platelets 1,000/mm <sup>3</sup>	298 (257 – 351)	305 (258 – 360)	0.17
Leukocytes 1,000/mm <sup>3</sup>	7.50 (6.50 – 8.90)	7.40 (6.20 – 8.60)	0.077
Lymphocytes 1,000/µL	2.60 (2.15 – 3.20)	2.60 (2.12 – 3.07)	0.20
Neutrophiles 1,000/µL	4.12 (3.35 – 5.07)	4.03 (3.20 – 5.02)	0.23
Monocytes 1,000/µL	0.46 (0.35 – 0.60)	0.43 (0.32 – 0.56)	0.003
<b>Quantitative IFN<math>\gamma</math> release assay result</b>			
IFN $\gamma$ Nil tube IU/L	0.15 (0.09 – 0.29)	0.14 (0.08 – 0.28)	0.042
IFN $\gamma$ TB-Nil tube IU/L	2.8 (1.1 – 6.7)	0.0 (0.0 – 0.1)	<0.001
IFN $\gamma$ Mitogen-Nil tube IU/L	9.32 (3.72 – 10.00)	8.68 (3.41 – 10.00)	0.53

Abbreviations: BCG, *Bacillus Calmette-Guerin*; BMI, body mass index; IQR, interquartile range.

<sup>a</sup> Median (IQR); %

<sup>b</sup> Mann-Whitney U test; Pearson's Chi-squared test; Fisher's exact test

<sup>c</sup> Diabetes defined as follows: no diabetes, random capillary blood glucose >101 mg/dL or hemoglobin A1c (HbA1c) <5.7%; prediabetes, HbA1c 5.7%–6.4%; diabetes, HbA1c ≥6.5.

753